NANO · MICRO small
www.small-journal.com

Light-Directed Liquid Manipulation in Flexible Bilayer Microtubes

*Bo Xu, Chongyu Zhu, Lang Qin, Jia Wei, and Yanlei Yu**

Flexible microfluidic systems have potential in wearable and implantable medical applications. Directional liquid transportation in these systems typically requires mechanical pumps, gas tanks, and magnetic actuators. Herein, an alternative strategy is presented for light-directed liquid manipulation in flexible bilayer microtubes, which are composed of a commercially available supporting layer and the photodeformable layer of a newly designed azobenzene-containing linear liquid crystal copolymer. Upon moderate visible light irradiation, various liquid slugs confined in the flexible microtubes are driven in the preset direction over a long distance due to photodeformation-induced asymmetric capillary forces. Several light-driven prototypes of parallel array, closed-loop channel, and multiple micropump are established by the flexible bilayer microtubes to achieve liquid manipulation. Furthermore, an example of a wearable device attached to a finger for light-directed liquid motion is demonstrated in different gestures. These unique photocontrollable flexible microtubes offer a novel concept of wearable microfluidics.

Flexible microfluidics provide a versatile toolbox for efficient, accurate, controllable, and high-throughput analytical measurements, which has potential applications ranging from wearable electronic devices for convenient digital lifestyle to biomedical devices that make conformal interfaces with the skin and internal organs.[1] Currently, the fabrication of the channels in flexible microfluidics suffers from complex processes evolving cleanroom-based photolithography or molding techniques to pattern microscale features on a planar substrate.[2,3] Lim and coworkers have shown that flexible microtube is an alternative modular component that can be easily assembled into various microfluidic devices.[4] This approach offers a feasible way for scaling up the production of flexible microfluidic systems. However, directional liquid transport in these flexible microtubes normally requires auxiliary control devices such as pumps and valves. Simplification of the existing microfluidic system is urgently required and still remains great challenges.[5–7]

Dr. B. Xu, Dr. C. Y. Zhu, Dr. L. Qin, Dr. J. Wei, Prof. Y. L. Yu
Department of Materials Science and State Key Laboratory of Molecular Engineering of Polymers
Fudan University
220 Handan Road, Shanghai 200433, China
E-mail: ylyu@fudan.edu.cn

The ORCID identification number(s) for the author(s) of this article can be found under https://doi.org/10.1002/smll.201901847.

DOI: 10.1002/smll.201901847

Stimuli-responsive deformable materials are able to change their shapes in response to external stimuli so that they have shown potentials for liquid manipulation in microsystems.[8–13] Photoresponsive azobenzene-containing liquid crystal polymers (LCPs) are of particular interest because light, compared to other stimuli, has unique advantages of local, temporal, precise, and remote control.[14–16] Azo LCPs produced fast, anisotropic, tunable and reversible photodeformation such as contraction,[17,18] bending,[19] oscillation,[20] walking,[21–23] twisting,[24,25] and waving.[26] In our previous work, we have fabricated a single layer microtube by azo linear liquid crystal polymer (LLCP) and present a conceptually novel way to propel liquids by asymmetric capillary force arising from photoinduced deformation of the microtube from a cylinder-like to cone-like geometry.[27] This strategy for photocontrolled liquid manipulation is expected to simplify microfluidics.

Herein, we report a follow-up strategy to propel various liquids by light toward the predetermined direction in a bilayer flexible microtube, which is capable of being changed into arbitrary shapes (trajectories). The photocontrollable flexible microtube (PFM) possesses a bilayer structure, including an outer flexible supporting layer and an inner photodeformable LLCP layer. The photoinduced reorientation of the azobenzene mesogens in the LLCP layer triggers the geometric change of the PFM and generates the asymmetric capillary force. Furthermore, several light-driven prototypes of parallel array, closed-loop channel and multiple micropump were established by the PFMs to achieve the liquid manipulation, demonstrating the potential applications in the fields of wearable microfluidics.

To overcome the resistance from the supporting layer, the LLCP layer requires robust mechanical properties and excellent deformability, transforming the microscopic structural change of mesogens to the macroscopic deformation of the bilayer. Thus, a newly designed azo-LLCP (polycyclooctene with azobenzene and biphenyl side chains at 1:2 ratio, PABBP, $M_n \approx 3.0 \times 10^5$ g mol^{-1}, $Đ \approx 1.67$) combining the photoresponsive azobenzene and biphenyl moieties was synthesized by ring-opening metathesis polymerization (**Figure 1**a; Figure S1, Supporting Information). The flexible backbone and long spacer of the copolymer PABBP provided enough free volume for the coassembly of the azobenzene and biphenyl mesogens, which have the similar molecular size. The results of 2D wide-angle

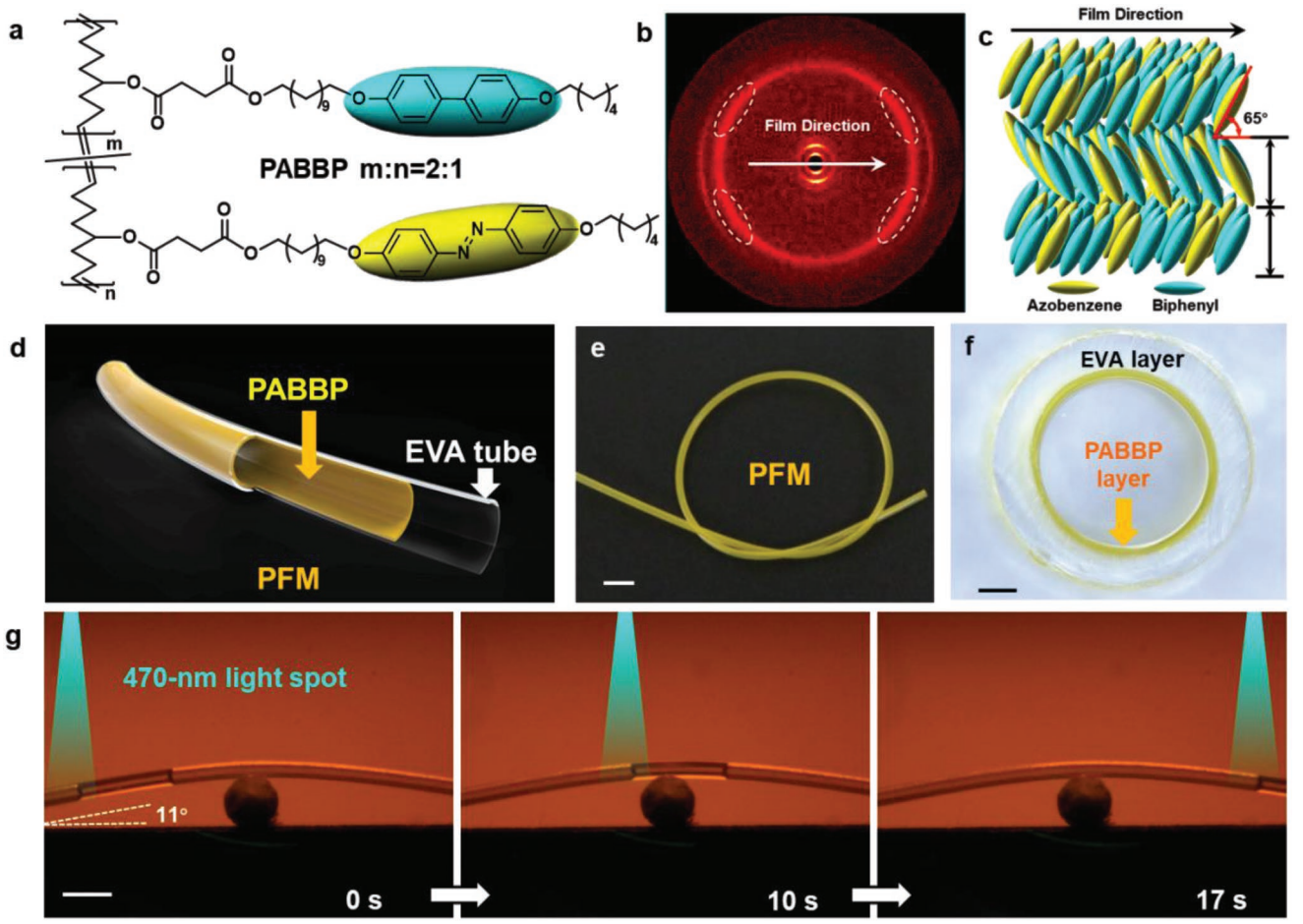

Figure 1. Design and characterization of PABBP copolymer and PFM. a) Chemical structure of the PABBP copolymer. b) 2D wide-angle X-ray diffraction pattern of the PABBP film. The X-ray beam was applied to the side of the film and parallel to the plane of the film. c) Illustration of the mesogen alignment in the PABBP film. d) Schematic representation of the bilayer structure of the PFM. e) Photograph of a knotted PFM showing good flexibility. The scale bar is 2 mm. f) Cross-section image of the PFM. The outer and inner diameters of the EVA microtube are ≈600 and ≈400 µm, respectively. The EVA layer is ≈100 µm thick and the PABBP layer is ≈25 µm thick. The scale bar is 100 µm. g) Photographs of the light-directed motion of an isopropanol slug climbing over a slope of 11° incline in a curved PFM. The intensity of the 470 nm point light was 120 mW cm^{-2}. The scale bar is 2 mm.

X-ray diffraction demonstrate that two kinds of the mesogens in the drop casting film spontaneously coassemble into a smectic C phase with the tilted angle of 65° in the lamellar layers after annealing at 60 °C (Figure 1b,c).

The tensile tests show that the drop casting film has robust mechanical property with 240 ± 25 MPa elastic modulus, which is ascribed to the ordered lamellar structure (Figure S2, Supporting Information). The incorporation of biphenyl mesogens increases the light penetration depth in the PABBP layer to enhance its photodeformability due to the cooperative effect of the two mesogens.[30] Upon local irradiation of 470 nm light with the intensity of 120 mW cm^{-2}, the single layer PABBP microtube generated an expansion because of the alignment change caused by the Weigert effect.[28] The exposed surface of the PABBP microtube was displaced toward the light at a maximum distance of 38 µm, which is two times larger than that of the azo-homopolymer microtube previously reported (Figures S3–S6 and Movie S1, Supporting Information).[27] The excellent photodeformability, self-assemble ability and moderate modulus make PABBP suitable to serve as the deformable layer to construct the bilayer PFM.

The commercially available ethylene-vinyl acetate (EVA) copolymer microtube (The outer and inner diameters are ≈600 and ≈400 µm, respectively, Supporting Information) was chosen as the supporting layer to assemble the PFM for its good flexibility and comparable modulus (≈70 MPa). The 1.5 m long bilayer PFM was then obtained through the inner surface coating of the EVA microtube with the 5 wt% dichloromethane solution of PABBP (Figure 1d; Figure S7, Supporting Information). The self-assemble ability of the mesogens in PABBP is of great benefit to the fabrication of the PFM without additional alignment steps such as surface anchoring,[29,30] stretching,[22,31] or photoalignment.[32]

Thanks to the good flexibility and mechanical properties of the EVA layer, one PFM can be knotted or hang a 200 g weight without damage (Figure 1e; Figure S7, Supporting Information). The cross-section of the PFM shows that the ≈100 µm thick EVA layer and the ≈25 µm thick PABBP layer are well composited, which is favorable to transport the deformation of the PABBP layer to the supporting EVA layer (Figure 1f). We used the 470 nm light spot (the illumination area was ≈0.2 mm^2

and the intensity was 120 mW cm^{-2}) to irradiate one end of the isopropanol slug confined in the PFM, driving the slug to move away from the light spot. Therefore, the slug was manipulated to move in a controllable direction and even climb over a slope of 11° incline at the speed of 0.4 mm s^{-1} (Figure 1g; Movies S2 and S3, Supporting Information). This experiment reveals that liquid transport performance is preserved under curved condition.

The photocontrolled asymmetric deformation of the PFM was clearly observed by a super resolution microscope. The exposed surface of the PFM was displaced toward the light by 15 µm upon local irradiation of the unpolarized 470 nm light with the intensity of 120 mW cm^{-2} (Figure S8, Supporting Information). The regional change in the PFM geometry from cylinder to conical structure was induced by the asymmetric expansion of the PABBP layer along the long axis of the microtube, creating the asymmetric capillary force to propel the liquid slug (**Figure 2**a).[27]

The moving speed of the confined liquid slugs gradually increased as the intensity of the 470 nm light increased (Figure 2b). Typically, wetting liquid with low viscosity was effectively propelled in the PFM with a fast moving speed. For example, both silicone oil and isopropanol were well wetted in the PFMs; however, the moving speed of isopropanol was faster than that of silicon oil at the same light intensity due to its lower viscosity. In the case of partially wetting liquids, such as water, the wettability of the inner surface was greatly enhanced by a hydrophilic composite gel layer;[27] therefore, water was successfully propelled in the PFM owing to the decrease of the contact angle from 94.5° to 9.2° (Figure S9, Supporting Information). When immersed in isopropanol, the PFM delivered the air bubbles upon 470 nm light (120 mW cm^{-2}) at the moving speed of 70 µm s^{-1} according to the same mechanism (Figure S10 and Movie S4, Supporting Information). Therefore, the PFMs are in theory able to propel any liquid with a suitable coating layer to change its wettability, showing advantage over other photocontrolled prototypes which only propel some specific fluids.[33,34]

Having established that light exerts precise control of liquid transportation, we prepared a parallel array of six PFMs to demonstrate their systematic performance (Figure 2c). Separate control of multiple liquid slugs was achieved by using point light sources and liquid manipulation in a single PFM had no influence on the others, showing more precise control than that in the magnetic tubular microactuators recently reported.[35] For example, the liquid slug in the second PFM was propelled to the left, while liquid slug in the fifth PFM moved to the right. Moreover, the liquid slugs in six PFMs were simultaneously propelled to the left when exposed to the line light and finally aligned along the direction of the line light (Movies S5 and S6, Supporting Information). The precise control of the liquid motion in parallel array reveals the possible integration of the PFMs to facilitate the assembly and miniaturization of the microfluidics.

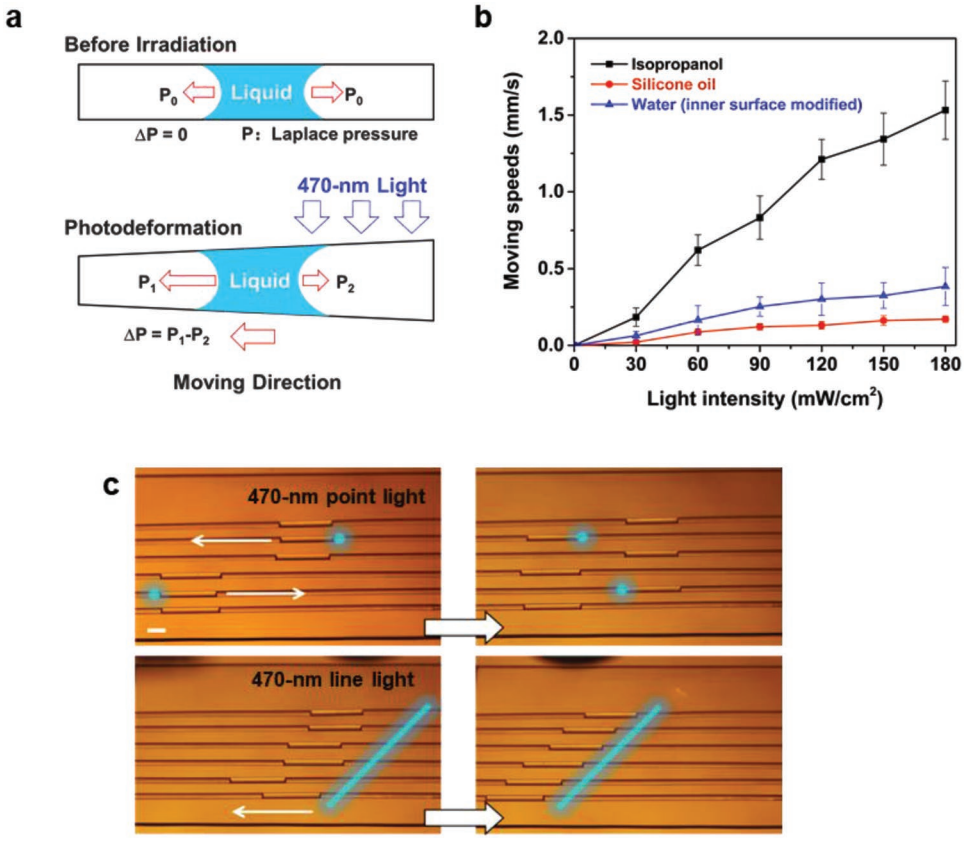

Figure 2. Mechanism of light-directed liquid transport. a) Schematic showing the transport mechanism of a liquid slug in the PFM upon 470 nm light irradiation. b) The plot of the moving speeds of three kinds of liquid slugs in the PFM or the wettability-modified PFM at different light intensities. c) Manipulation of isopropanol slugs in the PFM array by a point or line light with the intensity of 120 mW cm^{-2}. The scale bar is 5 mm.

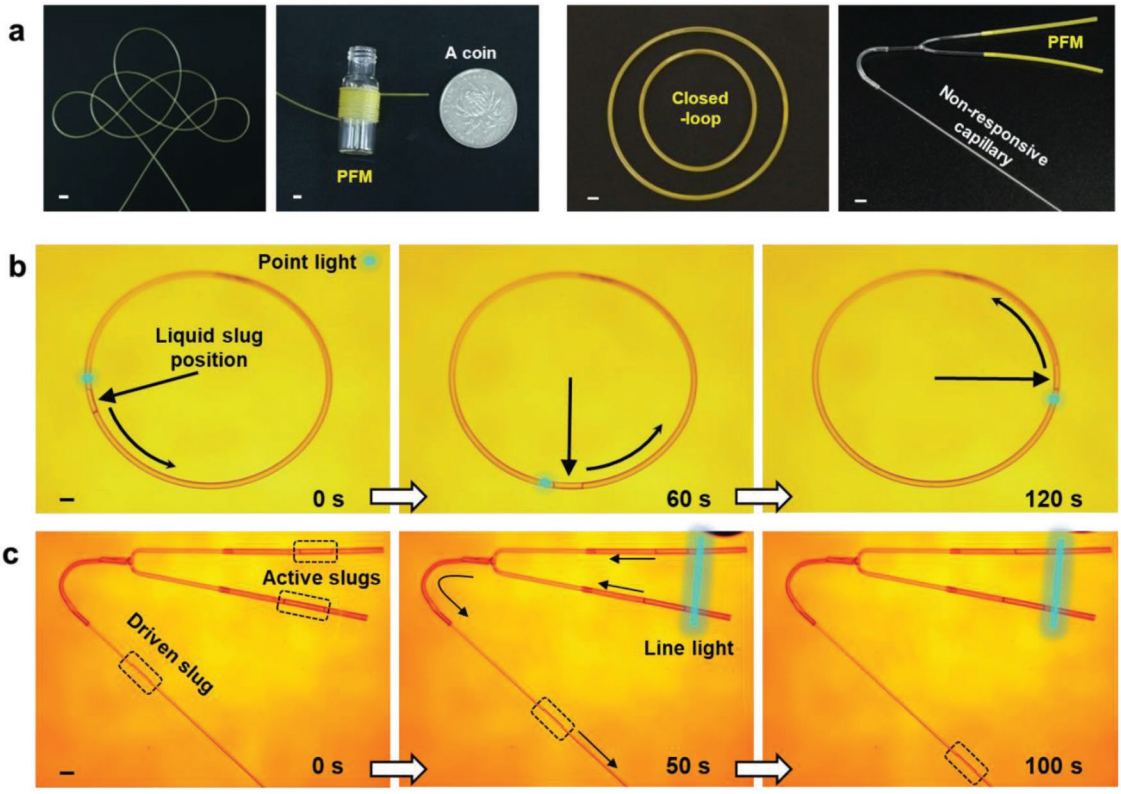

Figure 3. Photographs of the PFMs with different shapes and flexible actuators fabricated by the PFMs. a) Photographs of knot, coil, closed-loop actuator, and pumping system fabricated by the PFMs.The scale bars are 2 mm. b) Photographs of the closed-loop actuator fabricated of PFMs by end-to-end connection. 3 mL isopropanol is preloaded into the reactor. The light spot with an intensity of 120 mW cm^{-2} was located at the end of the confined slug. c) Photographs of a photocontrollable pump which was composed of two parallel PFMs. The intensity of the 470 nm line light irradiated on the active slugs was 120 mW cm^{-2}. The scale bars in (b,c) are 5 mm.

The PFM was facilely programmed into various shapes including knotted, spiral, and loop structures resulting from good flexibility (**Figure 3**a). Furthermore, the supporting EVA layer provides elasticity for tight connection between PFM themselves or other microtubes. A closed-loop microfluidic actuator was created with an airtight joint through the simple end-to-end connection of one PFM (Figure 3b; Movie S7, Supporting Information). Upon irradiation of 470 nm light, the inner isopropanol slug was propelled counterclockwise in the closed-loop actuator, where the liquid motion was hard to be driven by the conventional syringe pumps. This experiment reveals that the closed-looped PFM actuator is ideal for implementing biological reactions and analysis as it prevents solvent evaporation and contamination from the external environment.

Besides manipulating the inner liquids confined in the PFMs, the PFMs were also used as micropumps to drive the liquids in the external system. A "Y"-shaped glass capillary was incorporated with two PFMs and one nonresponsive microtube to serve as a pumping system. The preloaded 3 µL isopropanol slug in each PFM acted as the "liquid piston" and the 1 µL isopropanol in the nonresponsive microtube played the role of the "driven cargo" (Figure 3c; Movie S8, Supporting Information). The "liquid pistons" were driven by the asymmetric capillary forces arising from photodeformation of the PFMs, outputting positive or negative pressure to the nonresponsive microtube, where the "driven cargo" moved forward or backward respectively. Compared to the reported thermal-responsive micropump fabricated by contractile microspheres of LCPs,[11] this photocontrollable micropump demonstrates more precise and instantaneous actuation, and consequently shows superiority in constructing flexible microfluidics with high integration levels.

An example of liquid motion on fingers was demonstrated to explore the potential application of the PFM in wearable systems. The PFM that was attached to the index finger changed its trajectory accompanied with the different gestures (**Figure 4**a; Movie S9, Supporting Information). Under the 470 nm light with the intensity of 80 mW cm^{-2}, the liquid slug was manipulated away from or close to the fingertip in both straight and curved states (Figure 4b; Movie S9, Supporting Information). This feature is ascribed to the bilayer structure of the PFM, which is capable of being changed into arbitrary 3D shapes (trajectories) and preserves photodeformability to propel the inner liquids. Compared to high energy UV light, the 470 nm light is harmless to human body when biomedical application is taken into consideration; hence the PFM is suitable for building wearable and implantable microfluidic components.

It is well known that bilayer actuators suffer from delamination of the two layers after long-term repeating actuation in response to external stimuli, resulting in a decreased lifetime.[36] Wu and coworkers reported that a scratch on the azo polymer film was healed, which is based on UV light to trigger

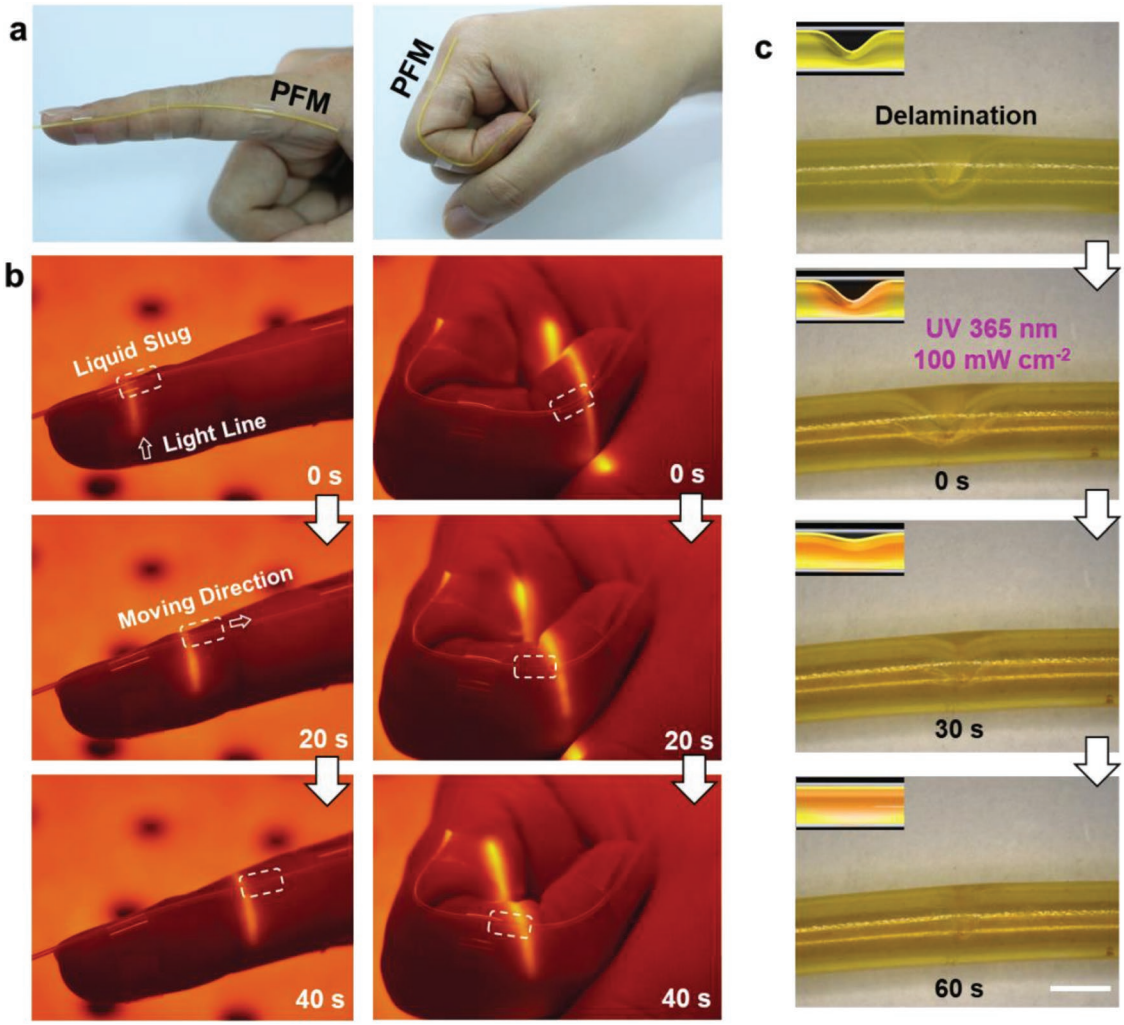

Figure 4. A wearable PFM showing liquid transport upon 470 nm irradiation light and self-healable property of the PABBP inner layer. a) Photographs of a PFM attached on the index finger. b) Photocontrolled transport of an isopropanol slug in the PFM upon the irradiation of 470 nm line light (80 mW cm^{-2}). c) Photoinduced self-healing of the PABBP inner layer. Inset: illustration of self-healing. The scale bar is 500 µm.

photofluidization.[37–39] As the glass transition temperature (T_g) of PABBP with *cis*-azobenzene was about 28 °C (Figure S16, Supporting Information), while the *trans*-azobenzene polymer has a T_g of 57 °C, the photofluidization mechanism could be applied to achieve the light-induced healing of the delaminated bilayer PFM made of PABBP. To demonstrate this, a delaminated bilayer PFM was prepared and repaired with the aid of UV and blue light irradiation. Upon the UV light irradiation (365 nm, intensity of 100 mW cm^{-2}) within 1 min, the damaged PABBP layer reattached to the supporting layer. A further blue light irradiation for 15 s allows the *cis*-to-*trans* isomerization of the azobenzene moieties and recovered the light-directed liquid propulsion of the repaired PFM (Figure 4c; Movie S10, Supporting Information), offering the PFMs with a longer lifetime. During the healing process, it was found that the temperature of the PABBP layer rise to around 40 °C, suggesting the photothermal effect of PABBP in combined with its T_g decrease contributes the success of the self-healing process.

In summary, we have reported a simple strategy to fabricate the visible-light-powered bilayer PFMs by coating the EVA supporting layer with novel PABBP photodeformable layer. One single PFM was able to transform into arbitrary shapes, including knot, helix, and serpentine. Upon 470 nm light, various liquid slugs in the PFMs were manipulated due to photodeformation-induced asymmetry capillary force. The unique PFMs were excellent candidates to simplify the complex flexible microfluidic systems. Several light-driven prototypes of parallel array, closed-loop channel and multiple micropumps were established by the PFMs to demonstrate systematic control and micropumping system. Furthermore, the photoinduced self-healing property of the PFMs enhanced their reliability in wearable and integrated microfluidic systems. We anticipate that these PFMs will find use in microelectromechanical systems (MEMS) and lab-on-a-chip settings as the photocontrollable components and liquid manipulation tools.

Supporting Information

Supporting Information is available from the Wiley Online Library or from the author.

Acknowledgements

This work was supported financially from the National Natural Science Foundation of China (21734003, 51573029, and 51721002), the National Key R&D Program of China (2016YFA0202902 and 2017YFA0701302), Innovation Program of Shanghai Municipal Education Commission (2017-01-07-00-07-E00027), Natural Science Foundation of Shanghai (17ZR1440100), and Science and Technology Commission of Shanghai Municipality (17JC1400200).

Conflict of Interest

The authors declare no conflict of interest.

Keywords

flexible actuators, liquid crystal polymers, liquid manipulation, photodeformation, self-healing

Received: April 11, 2019
Published online: May 7, 2019

[1] F. Wu, S. Chen, B. Chen, M. Wang, L. Min, J. Alvarenga, J. Ju, A. Khademhosseini, Y. Yao, Y. S. Zhang, J. Aizenberg, X. Hou, *Small* **2018**, *14*, 1702170.
[2] A. K. Au, W. Lee, A. Folch, *Lab Chip* **2014**, *14*, 1294.
[3] G. M. Whitesides, *Lab Chip* **2013**, *13*, 11.
[4] W. Xi, F. Kong, J. C. Yeo, L. Yu, S. Sonam, M. Dao, X. Gong, C. T. Lim, *Proc. Natl. Acad. Sci. USA* **2017**, *114*, 10590.
[5] J. Ter Schiphorst, J. Saez, D. Diamond, F. Benito-Lopez, A. Schenning, *Lab Chip* **2018**, *18*, 699.
[6] L. Dong, H. Jiang, *Soft Matter* **2007**, *3*, 1223.
[7] D. Baigl, *Lab Chip* **2012**, *12*, 3637.
[8] F. Benito-Lopez, M. Antoñana-Díez, V. F. Curto, D. Diamond, V. Castro-López, *Lab Chip* **2014**, *14*, 3530.
[9] S. R. Sershen, G. A. Mensing, M. Ng, N. J. Halas, D. J. Beebe, J. L. West, *Adv. Mater.* **2005**, *17*, 1366.
[10] C. H. Zhu, Y. Lu, J. Peng, J. F. Chen, S. H. Yu, *Adv. Funct. Mater.* **2012**, *22*, 4017.
[11] E. K. Fleischmann, H. L. Liang, N. Kapernaum, F. Giesselmann, J. Lagerwall, R. Zentel, *Nat. Commun.* **2012**, *3*, 1178.
[12] C. L. van Oosten, C. W. M. Bastiaansen, D. J. Broer, *Nat. Mater.* **2009**, *8*, 677.
[13] A. Sánchez-Ferrer, T. Fischl, M. Stubenrauch, A. Albrecht, H. Wurmus, M. Hoffmann, H. Finkelmann, *Adv. Mater.* **2011**, *23*, 4526.
[14] E. K. Fleischmann, R. Zentel, *Angew. Chem., Int. Ed.* **2013**, *52*, 8810.
[15] X. Qing, J. Lv, Y. Yu, *Acta Polym. Sin.* **2017**, *11*, 1679.
[16] T. J. White, D. J. Broer, *Nat. Mater.* **2015**, *14*, 1087.
[17] H. Finkelmann, E. Nishikawa, G. G. Pereira, M. Warner, *Phys. Rev. Lett.* **2001**, *87*, 15501.
[18] M. Li, P. Keller, B. Li, X. Wang, M. Brunet, *Adv. Mater.* **2003**, *15*, 569.
[19] Y. Yu, M. Nakano, T. Ikeda, *Nature* **2003**, *425*, 145.
[20] K. Kumar, C. Knie, D. Bléger, M. A. Peletier, H. Friedrich, S. Hecht, D. J. Broer, M. G. Debije, A. P. H. J. Schenning, *Nat. Commun.* **2016**, *7*, 11975.
[21] M. Yamada, M. Kondo, R. Miyasato, Y. Naka, J. Mamiya, M. Kinoshita, A. Shishido, Y. Yu, C. J. Barrett, T. Ikeda, *J. Mater. Chem.* **2009**, *19*, 60.
[22] X. Lu, S. Guo, X. Tong, H. Xia, Y. Zhao, *Adv. Mater.* **2017**, *29*, 1606467.
[23] J. J. Wie, M. R. Shankar, T. J. White, *Nat. Commun.* **2016**, *7*, 13260.
[24] M. Wang, B.-P. Lin, H. Yang, *Nat. Commun.* **2016**, *7*, 13981.
[25] S. Iamsaard, S. J. Aßhoff, B. Matt, T. Kudernac, J. J. L. M. Cornelissen, S. P. Fletcher, N. Katsonis, *Nat. Chem.* **2014**, *6*, 229.
[26] A. H. Gelebart, D. Jan Mulder, M. Varga, A. Konya, G. Vantomme, E. W. Meijer, R. L. B. Selinger, D. J. Broer, *Nature* **2017**, *546*, 632.
[27] J. A. Lv, Y. Liu, J. Wei, E. Chen, L. Qin, Y. Yu, *Nature* **2016**, *537*, 179.
[28] Y. Yu, T. Ikeda, *J. Photochem. Photobiol., C* **2004**, *5*, 247.
[29] T. Ikeda, M. Nakano, Y. Yu, O. Tsutsumi, A. Kanazawa, *Adv. Mater.* **2003**, *15*, 201.
[30] Y. Yu, T. Maeda, J. Mamiya, T. Ikeda, *Angew. Chem., Int. Ed.* **2007**, *46*, 506.
[31] J. Küpfer, H. Finkelmann, *Makromol. Chem., Rapid Commun.* **1991**, *12*, 717.
[32] L. T. de Haan, C. Sánchez-Somolinos, C. M. W. Bastiaansen, A. P. H. J. Schenning, D. J. Broer, *Angew. Chem., Int. Ed.* **2012**, *51*, 12469.
[33] H. Geng, K. Zhou, J. Zhou, H. Ma, C. Lv, C. Li, Z. Xu, L. Qu, *Angew. Chem., Int. Ed.* **2018**, *57*, 15435.
[34] K. Ichimura, *Science* **2000**, *288*, 1624.
[35] W. Lei, G. Hou, M. Liu, Q. Rong, Y. Xu, Y. Tian, L. Jiang, *Sci. Adv.* **2018**, *4*, eaau8767.
[36] T. Kamal, S.-Y. Park, *Chem. Commun.* **2014**, *50*, 2030.
[37] H. Zhou, C. Xue, P. Weis, Y. Suzuki, S. Huang, K. Koynov, G. K. Auernhammer, R. Berger, H. J. Butt, S. Wu, *Nat. Chem.* **2017**, *9*, 145.
[38] Y. Yue, Y. Norikane, R. Azumi, E. Koyama, *Nat. Commun.* **2018**, *9*, 3234.
[39] P. Weis, W. Tian, S. Wu, *Chem. - Eur. J.* **2018**, *24*, 6494.

